Research Square

Preprints are preliminary reports that have not undergone peer review.
They should not be considered conclusive, used to inform clinical practice,
or referenced by the media as validated information.

Neural Markers of Auditory Symbol Learning: Multiscale EEG Evidence from Morse Code Training

Zhongyang He
Information Engineering University
Ying Zeng
Information Engineering University
Hua Zhao
Information Engineering University
Li Tong
Information Engineering University
Shan Gao
University of Electronic Science and Technology of China
Yuanlong Gao
Information Engineering University
Yunying Qu
Information Engineering University
Changfu Pei
peichangfu1992@163.com
Information Engineering University
Bin Yan
Information Engineering University

Research Article

Keywords: Neural Markers, Auditory Symbol Learning, Morse Code, EEG

Posted Date: March 18th, 2026

DOI: https://doi.org/10.21203/rs.3.rs-9031528/v1

License: This work is licensed under a Creative Commons Attribution 4.0 International License.
Read Full License

Additional Declarations: No competing interests reported.

Neural Markers of Auditory Symbol Learning: Multiscale EEG Evidence from Morse Code Training

Zhongyang He [1,†], Ying Zeng [1,†], Hua Zhao [1], Li Tong [1], Shan Gao [2], Yuanlong Gao [1], Yunying Qu [1] , Changfu Pei [1,*], Bin Yan [1,*]

[1]Henan Key Laboratory of Imaging and Intelligent Processing, Information Engineering University, Zhengzhou 450001, China
[2]University of Electronic Science and Technology of China, Chengdu 610000, China
*Correspondence: peichangfu1992@163.com (Changfu Pei); ybspace@hotmail.com (Bin Yan)
[†]These authors contributed equally.

Neural Markers of Auditory Symbol Learning: Multiscale EEG Evidence from Morse Code Training

Abstract: To investigate how symbolic system learning induces neural plasticity, we examined the neural mechanisms of auditory symbolic processing using Morse Code (MC), a structured auditory symbolic system. In this study, novice learners underwent two months of MC training while electroencephalography (EEG) was recorded before and after training. We examined training-induced neural plasticity at two complementary levels: the local level and the global level. At the local level, MC training led to a significant decrease in N200 amplitude at the Fz electrode ($p < 0.05$), indicating reduced engagement of controlled processing and a shift toward more automated processing during the dot-count discrimination task (i.e., more efficient early task processing). At the global level, phase-locking value (PLV) analyses revealed a training-associated reorganization of task-evoked functional connectivity, with the right temporal T8 node showing increased hub-like centrality and network properties becoming more favorable for information integration and transmission. These findings suggest that, as a result of training, the brain's perception of rhythmic auditory stimuli has changed, reflecting both local processing optimization and global network reorganization. The findings were consistent with training-associated changes in task-evoked neural dynamics at both event-related potentials (ERP) and network levels, captured by candidate neural markers integrating ERP and network metrics.
Keywords: Neural Markers; Auditory Symbol Learning; Morse Code; EEG

I. Introduction

Symbolic systems acquisition exemplifies the remarkable plasticity of the human brain, involving multi-level functional reorganization and structural optimization(Schmidt-Wilcke et al., 2010; Lövdén et al., 2013). However, similar to language and music learning, symbol systems learning in natural contexts is typically prolonged and involves complex, interacting variables, making it difficult to achieve effective experimental control(Zatorre et al., 2007; Liu et al., 2021). To overcome this limitation, researchers often employ highly controllable artificial symbol systems as experimental paradigms. Morse Code (MC) encodes all characters using only two basic temporal units, “dot” and “dash.” While its physical structure is simple, it preserves the core combinatorial rules of symbolic systems and thus imposes multidimensional cognitive demands(Kujala et al., 2003). Mastering MC requires fine temporal discrimination, sustained attention, working memory, and rule-based decoding. Importantly, learners can usually achieve basic proficiency within several months, providing an ideal time window to track neural plasticity under strictly controlled conditions(Schlaffke et al., 2015).

Building on these advantages, many studies have adopted MC as a model symbolic system to investigate experience-dependent neural plasticity. For example, Schmidt-Wilcke et al. reported enhanced activity after training in brain regions related to language perception and memory(Schmidt-Wilcke et al., 2010),while Schlaffke et al. showed that MC learning can induce plastic adaptations in regions associated with reading and language(Schlaffke et al., 2015) and examined the role of white matter in language learning(Schlaffke et al., 2017). In addition, Kujala

et al. investigated the impact of MC learning on functional lateralization(Kujala et al., 2003), and Junker examined the role of multisensory experience in the decoding of non-lexical stimuli(Junker, n.d.). However, despite the millisecond-level temporal resolution of electroencephalography (EEG), which offers a unique advantage for capturing early neural dynamics during auditory symbol decoding(Näätänen & Picton, 1987), relatively few EEG studies have capitalized on this strength. Most have instead focused on later ERP components (such as P3a)(Uther et al., 2006), thereby failing to provide a comprehensive characterization of the multiscale neural plasticity processes induced by MC training.

To more effectively leverage EEG to capture brain plasticity induced by symbolic system learning, we analyzed neural changes at two complementary levels: the local level and the global level. At the local level, event-related potentials (ERP) reflected temporally precise processing within specific cortical regions and thus provided a powerful tool. In the present study, we focused on the N200 component of ERP, which typically emerged around 200 ms after stimulus onset and was closely associated with auditory discrimination and attentional modulation(Folstein & Van Petten, 2008; Zou et al., 2019). In the context of MC learning, N200 can serve as a key index of early perceptual encoding efficiency(Patel & Azzam, 2005). At the global level, learning-induced neural reorganization is also reflected in dynamic changes in patterns of brain network connectivity(Klug et al., 2022). Phase-locking Value (PLV) can be used to quantify oscillatory synchrony between brain regions and thereby construct functional connectivity networks(Pei, Huang, et al., 2023); combined with graph-theoretical analysis, this allows for further characterization of network organization in terms of segregation, integration, efficiency, and lateralization(Bullmore & Sporns, 2009). Notably, studies on rhythm and prosody in auditory processing have shown that rhythm-dominant auditory stimuli (such as speech envelopes, prosody, and musical rhythms) tend to elicit right-hemisphere dominance, which may reflect the leading role of the right hemisphere in processing temporally organized auditory information(Abrams et al., 2008; Oechslin et al., 2018). However, there is still a lack of research that systematically examines MC learning from the combined perspectives of ERP and brain network analysis, and it remains unclear how training reshapes the organizational patterns of information-processing networks in the brain.

To address these gaps, this study employed EEG to systematically investigate how MC training modulates the early processing of auditory rhythmic symbols and the reorganization of functional brain networks. A total of 22 MC-naïve university students were randomly assigned to a experimental group and a control group. The training group received two months of auditory MC recognition training, whereas the control group received no intervention. All participants completed behavioral tests and EEG recordings both before and after the training period (the control group was tested with the same time interval). This study primarily investigates the changes in participants' perception of rhythmic patterns in MC after training, rather than the decoding of MC.

Based on previous research, we proposed the following hypotheses. H1: The experimental group will demonstrate greater accuracy and shorter reaction times in the MC recognition task after training. H2: MC training will lead to significant changes in N200 amplitude, indicating enhanced efficiency in early perceptual encoding. H3: MC training will induce reorganization of PLV functional networks, potentially accompanied by changes in hemispheric lateralization patterns associated with rhythm-related information processing.

II. Materials and Methods

1.Participants

22 participants (all male, average age 22.12 ± 1.78 years) have been recruited for the study and all are right-handed with normal hearing. The 22 participants were all undergraduate students with no prior experience in MC and have sufficient time to participate in MC training. None of the participants had any history of using psychoactive substances, and no reports of personal or family history of mental or neurological disorders from them. 22 participants were randomly selected and assigned to two groups: 12 in the experimental group, drawn from a class learning MC, received two months of auditory identification training for MC; the other 10, in the control group, were selected from a class not studying MC and received no training related to MC aside from their participation in the experiment. The participants were informed of the content of the experiment beforehand and have signed an informed consent statement prior to the experiment. The sample size and homogeneity of the participants were limited due to the specific nature of the MC auditory identification task, as it is challenging to recruit individuals who are engaged in related work. This study adhered to the Declaration of Helsinki and has been approved by the Ethics Committee of University of Electronic Science and Technology of China (No. 106412023030125880).

2.Stimuli

The experimental stimulus material consisted of authentic MC audio for the 26 English characters (as shown in Figure 1), where “dot” was 1 unit length and “dash” 3 units lengths, with one unit length interval between dots and dashes within a character. The 26 characters had five options for the number of “dots” ranging from 0 to 4, and four options for the number of “dashes” ranging from 0 to 3. In this paper, the number of letters transmitted per minute has been defined as the code speed, referred to as Character Per Minute (CPM). The experiment includes three code speeds (15, 30, and 40 CPM), which were determined based on actual training objectives in the course. These rates serve as a dynamic difficulty adjustment mechanism, enabling a stepwise manipulation of task demands through speed-graded stimuli. The playback duration of each character stimulus material has been determined by the different code speeds, with the stimulus duration range for 40 CPM being 72 ms to 936 ms, and correspondingly longer durations for 30 and 15 CPM.

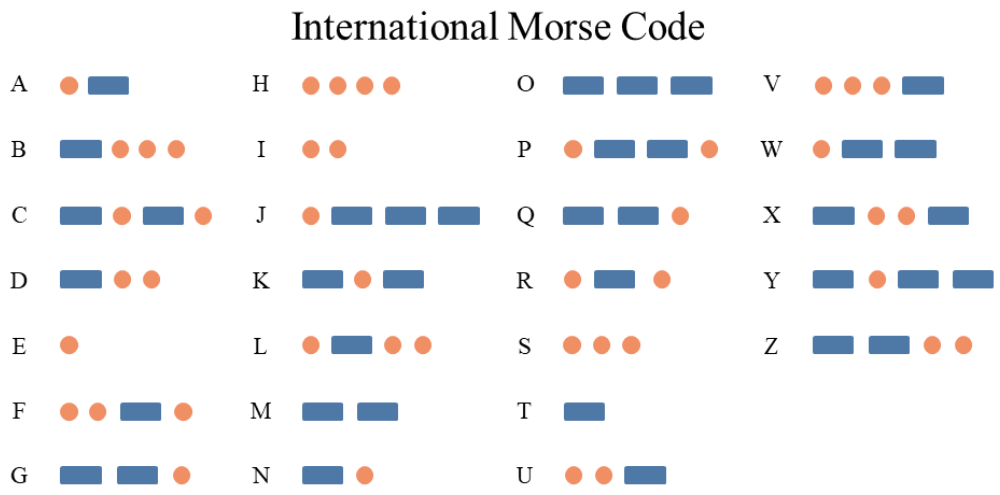


Fig. 1. International Morse Code. The circle stands for dot and the box stands for dash.

3. Procedure

The experiment consisted of three parts: Session A, Session B, and Session C, corresponding to Data Collection, MC Training, and Data Collection, respectively (see Figure 2). Participants in the experimental group took part in all three sessions. Session B, the MC training, was integrated into the experimental group participants' required coursework. They were required to complete at least 40 hours of MC training over a two-month period. Following the training, they had to pass a proficiency test achieving an accuracy rate exceeding 70% at 40 CPM. Participants in the control group only participated in Session A and Session C. The two data collection sessions were conducted two months apart, with the control group's sessions scheduled in parallel with those of the experimental group. All participants completed two data collection sessions, which corresponded to the Pre- and Post-training phases for the experimental group (Sessions A and C).

We designed an experimental paradigm using authentic MC communication signals to collect EEG data, thereby enhancing the ecological validity of our findings and ensuring their direct relevance for future applications in real-world monitoring(Chiang et al., 2023).

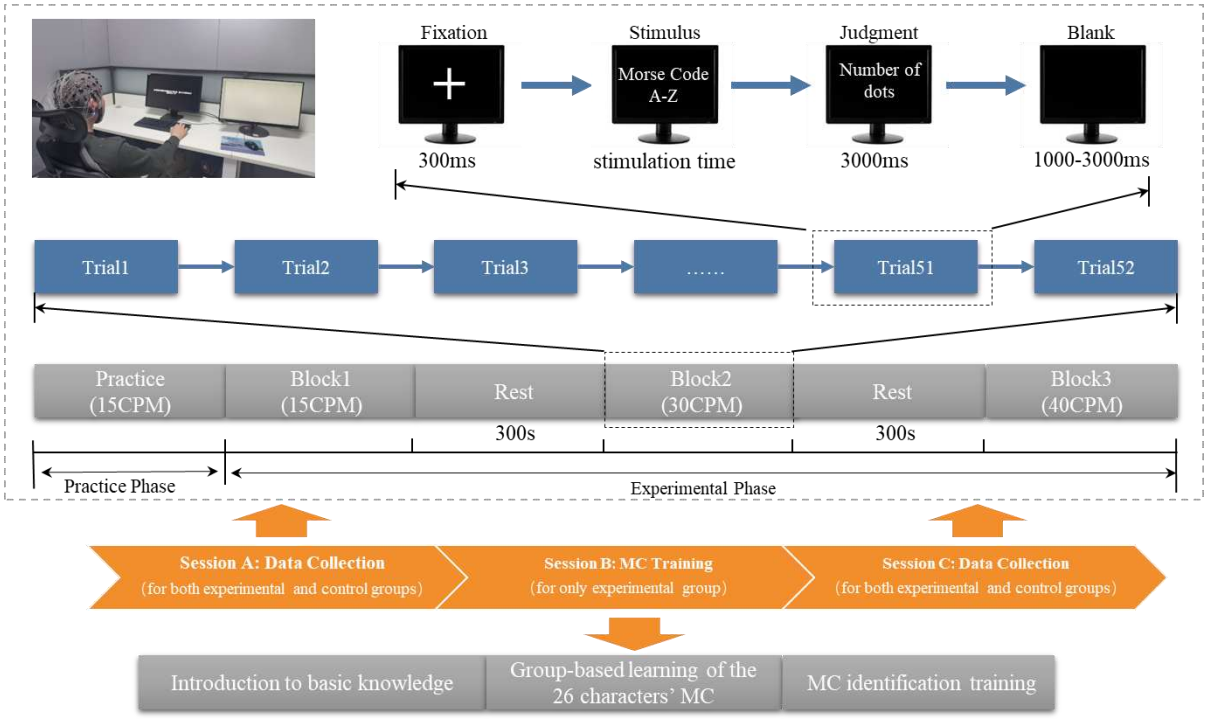


Fig. 2. Schematic diagram of the experimental process for the experimental and control groups.

The data collection session consists of two phases: the practice phase and the experimental phase. The practice phase was designed to familiarize the participants with the basic experimental procedures. The experimental phase was divided into three blocks, with each block corresponding to one code speed. Each block contained 52 trials, and each trial consisted of one MC audio stimulus for an English character. The 26 characters were randomly displayed twice, resulting in a total of 52 MC audio stimuli for each block. The specific experimental procedure was as follows:

- **Experimental Preparation**: Before the experiment, participants were informed of the precautions, operational procedures, and the code speeds of the MC to be delivered in each block.
- **Practice Phase**: Once the participants were fully prepared, they could start the experiment by pressing any

key. Each participant practiced 10 trials in the practice phase. The stimulus materials during the practice phase used MC at a speed of 15 CPM.

- **Experimental Phase**: Each trial started with a white cross displayed for 300 ms, followed by MC audio stimuli. Participants listened to the stimuli without making any movement and were encouraged to remain as still as possible. Based on pre-experimental findings, it was noted that the "dot" sound was shorter, and more challenging to judge than the "dash" sound. Therefore, the participants were required to judge and to response the number of "dots" they had heard. Among the 26 English letters mapped to MC, the number of dots exhibits five distinct distributions ranging from 0 to 4. Participants response any those five number to complete the task. The judgment phase had a maximum duration of 3,000 ms, the trial advanced to a blank screen either after participant input or timeout. The black screen lasting between 1000 to 3000 ms presented randomly.

The experimental paradigm was programmed using E-Primer3.0 software.

4. Data Collection

During the experiment, participants sat comfortably in a quiet, shielded room. When collecting EEG data, the stimuli were presented to the participants through external speakers, and they were instructed to avoid significant head movements to ensure the quality of the collected data. During the data collection phase under task conditions, participants were required to focus their attention, listen carefully to the stimuli, and respond based on their judgment.

The experiment utilized a 64-channel HIamp active electrode EEG cap and g.Recoder software from g.tec, Austria, to collect EEG signals. The sampling rate was set at 600 Hz, and the filter range was set to [0.1 Hz, 100 Hz]. A notch filter was applied at 48 Hz-52 Hz to eliminate the influence of power frequency interference. The EEG data collection included 64 channels, with channel 63 connected to the right earlobe as reference electrode and channel 64 left empty. The remaining effective EEG signal channels (channels 1-62) were used for subsequent analysis, with AFz connected to GND.

5. Data Processing

In this study, MATLAB software (version R2018a) has been used to process the EEG data collected Pre- and Post-training. The data processing workflow was shown in Figure 3, which mainly includes four steps: behavioral data analysis, EEG data preprocessing, ERP analysis, and brain network analysis. This study focuses on changes in brain information processing before and after MC training. The effects of different code speeds are not analyzed, as combining data across speeds was prioritized to increase statistical power given the small sample size.

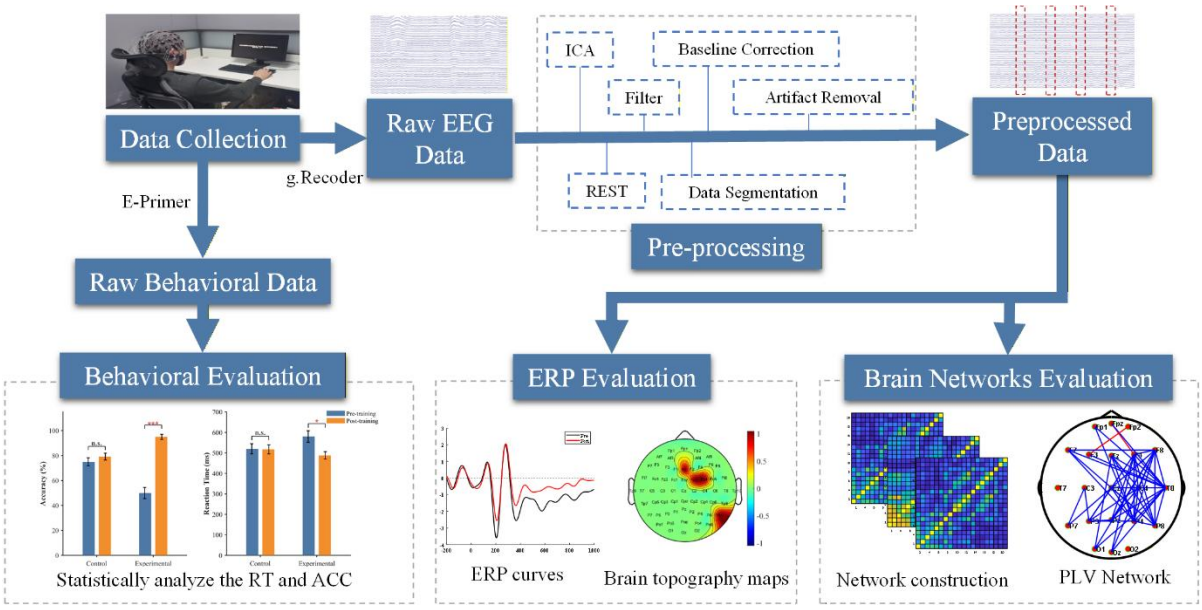


Fig. 3. Data collection and processing flow for the experimental and control groups.

(1) Behavioral Data Analysis

Behavioral performance was assessed using reaction time (RT) and accuracy (ACC), which were extracted using E-Primer 3.0. Prior to statistical analysis, the distributions of RT and ACC for each condition were evaluated using the Lilliefors-corrected normality test. The results indicated that both measures conformed to a normal distribution; therefore, parametric tests were applied. For within-group comparisons, paired-samples t-tests (two-tailed, $\alpha = 0.05$) were conducted separately for the training and control groups to examine Pre- versus Post-training differences in RT and ACC.

(2) EEG Data Preprocessing

For all participants, the raw EEG data from the 62 channels were preprocessed according to the following steps.

- **Eye Movement Removal**: In this study, the FastICA algorithm was used to decompose the EEG signals into 62 independent components(Pion-Tonachini et al., 2019). After selecting and removing the artifact components, typically there is one artifact component, the EEG signals free from artifact interference were reconstructed. Ultimately, the rejection rate of components via ICA was 1.61%.
- **Re-referencing Calculation**: The data were re-referenced using the Reference Electrode Standardization Technique (REST) proposed by Yao et al.(Yao, 2001; Yao et al., 2019), which estimates a neutral reference at infinity via a forward head model. This approach was adopted to minimize the bias inherent in physical reference electrodes and to improve the comparability of EEG data across studies.
- **Signal Filtering**: During ERP analysis, a 1-10 Hz bandpass filter was applied; for the brain network analysis, a 1-40 Hz bandpass filter was used.
- **Data Segmentation**: The continuous EEG data were segmented based on the stimulus events into several equal-length segments. In this study, the onset of the experimental stimulus was set as the 0-time point, and the EEG data were divided into many segments, each spanning from 200ms before the 0-time point to 1000 ms after the point. Each block contained 52 trails, so an experiment contains 156 epochs.

- **Baseline Correction**: This step was used to calculate relative changes in EEG signals compared to a pre-stimulus mean. The data from 200 ms before the 0-time point were used as the baseline, assuming that the EEG signals before the 0-time point represented spontaneous EEG at the time of stimulus reception. By subtracting the average value of the data points before the 0-time point from the data after the 0-time point, part of the spontaneous EEG noise was eliminated.
- **Artifact Removal**: The artifact rejection threshold was set at ±120 μV, consistent with commonly used criteria in ERP research(Luck, 2005). Segments with amplitudes greater than the threshold were defined as bad segments and were completely removed. When preprocessing with a 1-10 Hz bandpass filter, 705 of 6,864 trials were rejected (10.27%). While a 1-40 Hz bandpass filter, 1,688 trials were removed (24.59%).

(3) ERP Analysis

This study focused on the changes in ERP Pre- and Post-training, as well as across different code speeds. The time window for the N200 component was selected to be 150-250 ms(Balconi & Vanutelli, 2016).

We compared the changes in the N200 component between the experimental and control groups. The analysis focused on three aspects: topographical maps of the N200 component at Pre- and Post-training; statistical analysis of the difference in N200 topographical maps between Pre- and Post-training; changes in N200 amplitude. The difference topographical maps were obtained by performing electrode-wise paired-samples t-tests (two-sided, $\alpha = 0.05$, FDR correction) on the mean ERP amplitudes within the N200 time window Pre- and Post- training, and binarizing the resulting *p*-values (1 = significant, 0 = non-significant) to identify electrodes showing significant differences. For these electrodes, additional subject-level t-tests (two-sided, α=0.05) were conducted and the corresponding ERP waveforms were plotted. These results were not only used for comparisons of ERP waveforms, but were also combined with changes in the N200 component to examine how MC training modulates the neural mechanisms underlying information processing.

To investigate the relationship between behavioral performance and changes in N200 amplitude, Pearson, Kendall's tau-b, and Spearman's rho correlation analyses were performed to assess the associations between behavioral indices (e.g., accuracy and reaction time) and N200 amplitude changes.

(4) Brain Network Analysis

To examine large-scale functional network changes associated with the experimental manipulation, we constructed PLV brain networks using EEG data. During the data preprocessing stage, a band-pass filter with a 1-40 Hz frequency range was applied. PLV was computed using the Hilbert transform, yielding values ranging from 0 to 1 that index the degree of phase synchronization between pairs of signals.

In order to reduce computational load and the complexity of brain network connections, as well as to mitigate the impact of the volume conduction effect(F. Li et al., 2016), this study adopted the standards used in previous research and selected 21 typical EEG electrodes distributed across the entire brain: Fp1, Fpz, Fp2, F7, F3, Fz, F4, F8, T7, C3, Cz, C4, T8, P7, P3, Pz, P4, P8, O1, O2, Oz(Murias et al., 2007; Xu et al., 2014; Zhang et al., 2021). We computed the PLV between every pair of EEG channels for all participants and across all experimental blocks for each participant, resulting in one 21x21 connectivity matrices per participant. Based on these PLV connection matrices, we set the threshold to 0.05 and computed the PLV network difference maps for different code speeds as

well as the average across all code speeds before and after training. To quantitatively analyze network properties, we calculated the LI of the PLV network and assessed the degree of network lateralization using paired t-tests(two-sided, α = 0.05) and effect size analysis (Cohen's d) (See Appendix A)(Seghier, 2008). Inspired by graph-theoretical analysis, we further computed Degree Centrality (DC), Node Strength (NS), Betweenness Centrality (BC), Eigenvector Centrality (EC) and Participation Coefficient (PC) to identify key nodes within the PLV network (See Appendix B)(Rubinov & Sporns, 2010; Newman & Newman, 2018).

To further assess the training-induced changes in network properties, we computed the corresponding network metrics based on the PLV connectivity matrices. These attributes included Clustering Coefficient (CC), Characteristic Path Length (CPL), Global Efficiency (Ge) and Local Efficiency (Le). These four parameters were selected because they capture complementary aspects of brain network organization: CC indexes local segregation, CPL and Ge quantify global information integration, and Le reflects the robustness and efficiency of information processing within local subnetworks, together providing a comprehensive characterization of PLV network reconfiguration. The calculation methods for the four network properties are provided in Appendix C(Zhang et al., 2021). We used an alpha level of 0.05 and tested the pre-post differences in the four metrics of network using paired-sample t-tests, or Wilcoxon signed-rank tests when normality was violated.

III. Experimental Results

1.Behavioral Data Analysis

In the behavioral data analysis, we focused on comparing the patterns of change in mean ACC and RT between the experimental and control groups.

(1) Behavioral Results of the Experimental and Control Groups

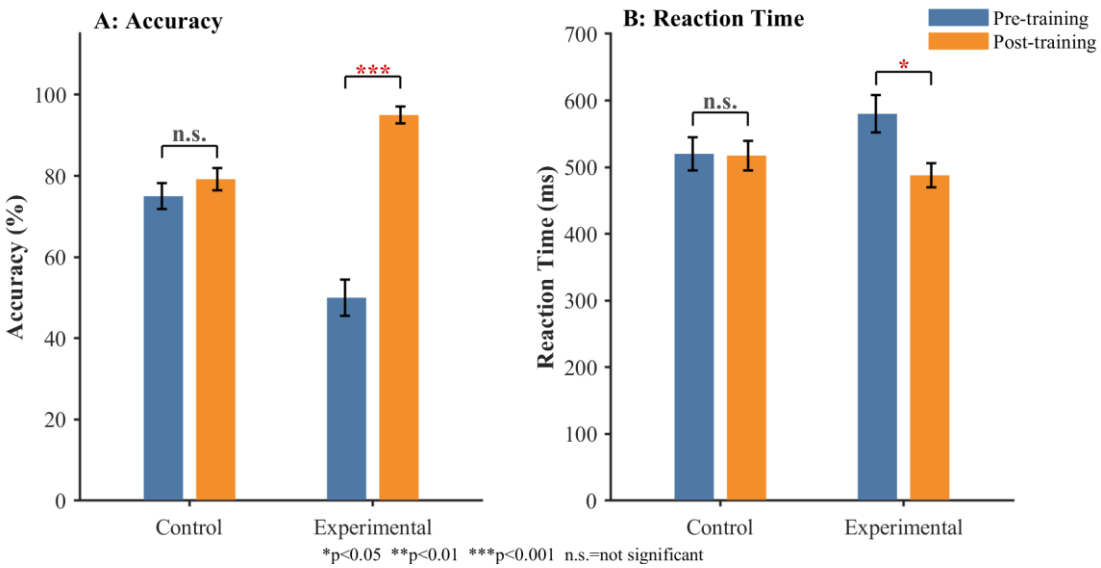


Fig. 4. Statistical comparison of mean ACC and RT between the experimental and control groups.

As shown in Figure 4, in terms of ACC, the experimental group exhibited a significant improvement after training ($p < 0.001$), with an increase of 45.0%. In contrast, although the control group showed a slight increase in accuracy between the two tests (an improvement of 4.2%), this change did not reach statistical significance (p =

0.355). Regarding RT, the experimental group responded significantly faster after training ($p < 0.05$), with an improvement of 15.9%. In the control group, however, the RT did not show a significant change ($p = 0.971$).

2.ERP Analysis

This section focuses on analyzing the ERP changes Pre- and Post- training in both the experimental and control groups, as well as the correlation between behavioral data and N200 amplitude in the experimental group.

(1) Comparison of N200 Between the Experimental and Control Groups

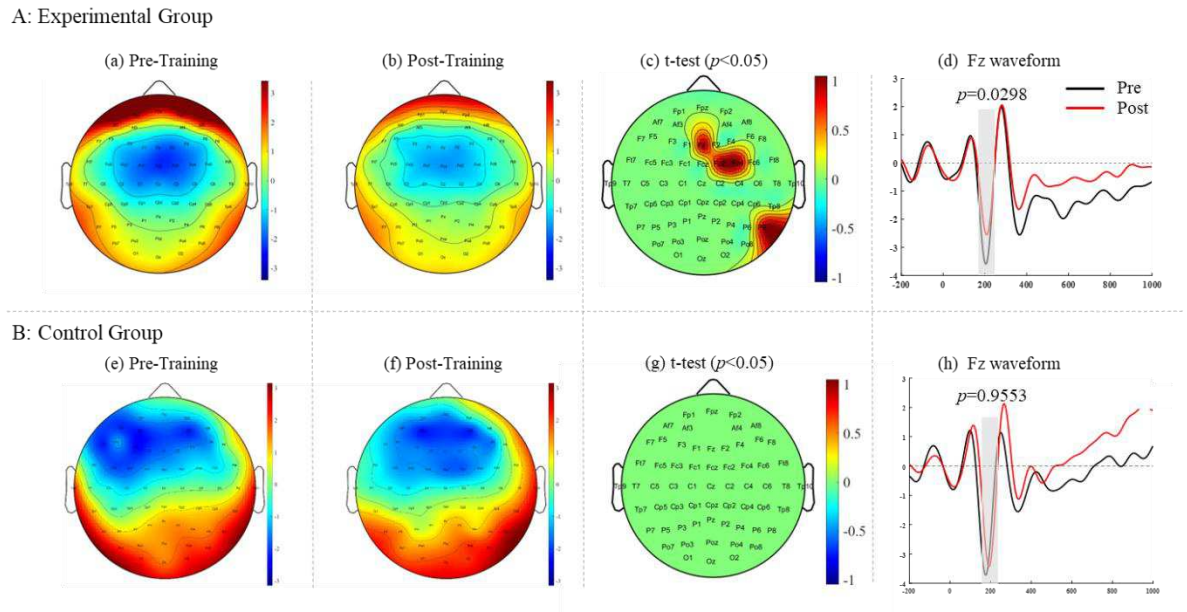


Fig. 5. A comparison of N200 topographic maps and statistical differences between the experimental and control groups before and after training. (A) Experimental Group: (a, b) topographical maps of the N200 component at Pre- and Post-training; (c) difference topographical maps of N200 between Pre- and Post-training ($p < 0.05$, FDR corrected); (d) ERP waveforms at the Fz electrode. (B) Control Group: (e, f) topographical maps of the N200 component before and after the equivalent time interval; (g) difference topographical maps of N200 between Pre- and Post-training ($p < 0.05$, FDR corrected). (h) ERP waveforms at the Fz electrode.

Figure 5 illustrated the changes in the N200 component between Pre- and Post- training in the experimental and control groups. As shown in Figure 5(a), (b), (e), and (f), the main activation of the N200 component in both groups was localized over the frontoparietal region and the parietal lobe, which is consistent with previous findings(Crowley & Colrain, 2004; Luck, 2005). After training, the activation in the frontoparietal region decreased in the experimental group (i.e., the absolute values of the negative potentials at the corresponding electrodes were reduced), whereas no obvious changes were observed in the control group. Figures 5(c) and 5(g) present the t-test results of the whole-brain N200 topographical maps. The results show that, in the experimental group, the N200 component exhibited significant differences between Pre- and Post-training at four electrodes: Fz, FC2, FC4, and P8 ($p < 0.05$). In contrast, no significant differences were found between the two sessions in the control group. Based on these results, we selected the Fz electrode as a representative site to further examine the waveform changes of the N200 component(Pei, Qiu, et al., 2023). As shown in Figures 5(d) and 6(h), the N200 amplitude at Fz in the experimental group was significantly reduced after training ($p < 0.05$), which is consistent with the decreased ERP activation over the frontal regions observed in the topographical maps. By contrast, the N200 component at Fz in the control group did not show

any significant change between Pre- and Post-training (p = 0.9553). While the N400 component is typically associated with semantic processing, this study primarily focuses on the brain's sensitivity to rhythmic patterns in auditory symbols. In the experimental group, we observed a reduction in the amplitude of the post-N400 components, suggesting a potential modulation of the neural processing dynamics due to the training. This change may reflect an adaptation to the rhythmic stimuli rather than semantic processing, as our task emphasized rhythmic symbol discrimination. As such, although the post-N400 components show differential patterns, we do not emphasize these findings in the context of semantic processing, as they are outside the scope of the current investigation.

Figure 5 showed that training-induced changes in the N200 component were found only in the experimental group, suggesting that MC training specifically modulated early cortical information processing.

(2) Correlation Between Behavioral Data and N200 Amplitude in the Experimental Group

To examine the relationship between training-induced changes in behavioral performance and changes in N200 amplitude, we conducted correlation analyses on the overall change scores within the experimental group (see Table 1).

Table 1. Correlation coefficients between behavioral changes and AM index changes.

Variable Pair	Pearson $r(p)$	Kendall's $\tau(p)$	Spearman's $\rho(p)$
△ACC&△AM	-0.202(0.265)	-0.246(0.135)	-0.291(0.179)
△RT&△AM	-0.547(0.033*)	-0.242(0.136)	-0.392(0.104)

The results showed a significant negative correlation between changes in reaction time (△RT) and changes in N200 amplitude (△AM) (Pearson r = -0.547, one-tailed p = 0.033), indicating that greater improvements in reaction time (larger reductions in RT) were associated with more pronounced changes in N200 amplitude. In contrast, the correlations between changes in accuracy (△ACC) and changes in N200 amplitude did not reach statistical significance (all one-tailed p > 0.10). The nonparametric Kendall's Tau-b and Spearman's Rho correlation analyses also did not reveal additional significant associations, and overall converged with the conclusions drawn from the Pearson correlation.

3.Brain Network Analysis

In this section, we first compared the Pre- and Post-training PLV network changes between the experimental and control groups. We then employ graph-theoretical analyses to quantitatively characterize the PLV network reorganization within the experimental group. Finally, we examine the training-related alterations in the experimental group's network attributes.

(1) Changes in the PLV network in the experimental and control groups

We first compared the differential PLV brain network, *LI* and PLV connection strength between the experimental and control groups, as shown in Figure 6.

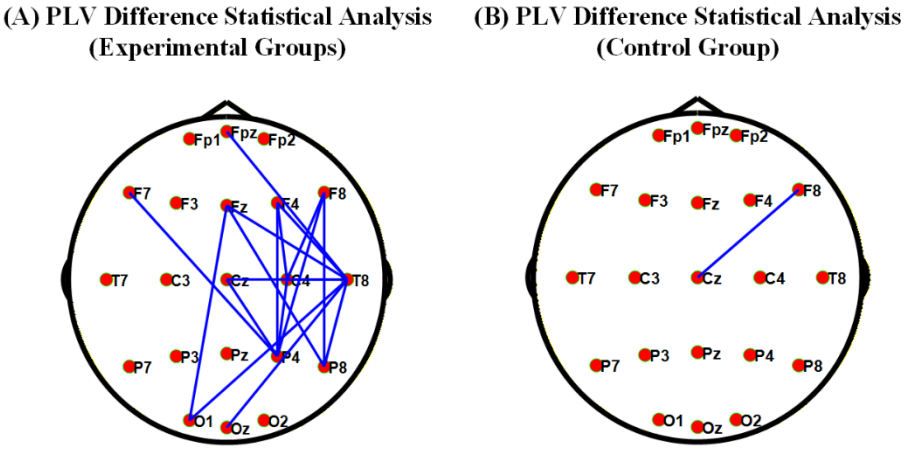


Fig. 6. Differences in PLV network patterns between experimental and control group. (A) The PLV difference statistical analysis in brain network patterns of the experimental groups, and blue lines indicate strengthened connections ($p < 0.01$, FDR corrected). (B) The PLV difference statistical analysis in brain network patterns of the control group ($p < 0.01$, FDR corrected).

As shown in Figure 6(A), in the experimental group the connectivity of the right hemisphere in the PLV network was significantly enhanced Post- training compared with Pre-training ($p < 0.01$), exhibiting a clear right-lateralized pattern. This suggested cortical reorganization following MC training and was consistent with the findings reported by Mankel and Oechslin(Mankel et al., 2022; Oechslin et al., 2018). To verify this lateralization effect, we calculated the *LI* for both the experimental and control groups using the method described in Appendix A. For the experimental group, the LI decreased from -0.0031 (± 0.0124) before training to -0.0160 (± 0.0163) after training, corresponding to a change rate of -412.3%, and a Cohen's d of -0.889 indicates a large effect(Panjeh et al., 2023). In addition, a paired t-test (one-tailed) on *LI* at the subject level revealed a significant difference between Pre- and Post-training ($p < 0.01$). For the control group, we applied the same analytical procedure. As shown in Figure 6(B), the differential statistical analysis of the PLV network connectivity revealed that only one connection line showed a significant change between the two measurement sessions. Meanwhile, the *LI* changed only slightly, from 0.0075 (± 0.0087) to -0.0002 (± 0.0090), with a change rate of −102.6%. The pre-test *LI* values greater than 0 could be attributable to inter-subject variability; however, the *LI* decreased after participants became familiar with the experimental task.

(2) Graph-theoretical analysis of PLV network in the Experimental Group

As shown in Figure 6(A), in the experimental group, the PLV network after training is organized around the temporal T8 region as a hub node, with its functional connections to the frontal and occipital lobes markedly strengthened. We computed graph-theoretical metrics of the PLV network in the experimental group following the procedures described in Appendix B. Following previous graph-theoretical studies that defined hubs as nodes whose centrality ranks fall within the top quantiles of the distribution (e.g., top 20% of degree centrality) in either biological or brain networks(X. Li et al., 2023; Song et al., 2022), We defined a node as a hub if at least three of its graph-theoretical metrics ranked within the top 50% among all nodes. The corresponding results were presented in Figure 7.

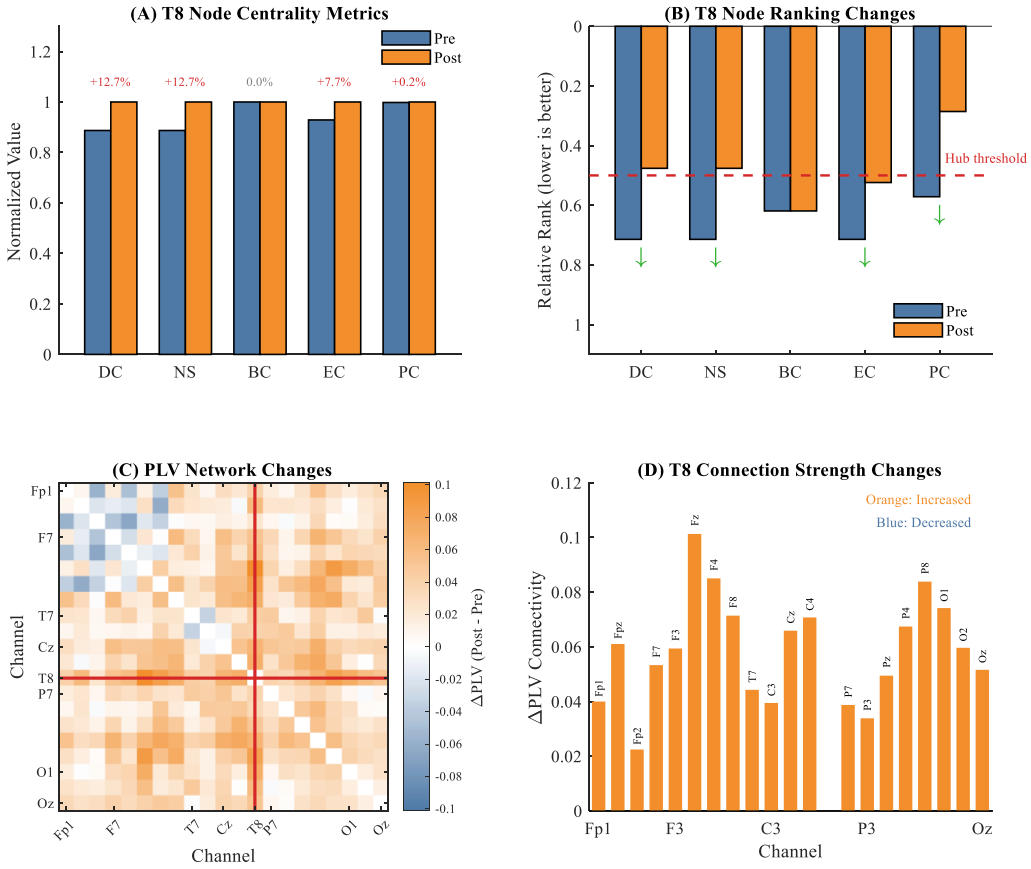


Fig. 7. Changes in the T8 node and network connectivity properties Pre- and Post-training. (A) Changes in multiple centrality metrics of the T8 node after training; (B) Changes in the ranking of the T8 node ranking; (C) Differences (post vs. pre) in the brain functional network characterized by PLV; (D) Changes in the strength of specific connections between the T8 node and other brain regions.

At the nodal level, group-averaged results indicate an increase in the centrality of the T8 node.. As shown in Figure 7A, the normalized values of four centrality metrics (DC, NS, EC, PC) for the T8 node increased after training, with DC and NS showing the most pronounced improvement (+12.7%), while BC remained unchanged. Correspondingly, the relative ranking of the T8 node within the whole network also improved positively (Figure 7B): the number of metrics entering the top 50% increased from 0 before training to 3 after training, indicating that the training effectively enhanced the node's importance within the network.

At the network connectivity level, the training induced a functional reorganization centered around the T8 node. The heatmap of the PLV connectivity matrix (Figure 7C) revealed widespread changes in the connection patterns corresponding to the row/column of the T8 node after training, manifested as enhanced connections (warm colors) with other brain regions. Further analysis of the direct connections of the T8 node (Figure 7D) corroborated this trend, showing strengthened connectivity with multiple channels (e.g., Fz, P8) to varying degrees, with some connections exhibiting particularly notable increases.

(3) Comparison of PLV Network Properties Pre- and Post- Training in the Experimental Group

To further validate the training-induced changes in network properties, we conducted comparative tests on the Pre- to Post-training differences in four network metrics: CC, CPL, Le, and Ge. Both paired sample t-tests and Wilcoxon signed-rank tests revealed statistically significant differences in three network properties (CC, CPL, and Le) between the Pre- and Post-training (**$p < 0.01$). Although Ge did not show a significant difference, it exhibited an increasing trend after training, as shown in Figure 8.

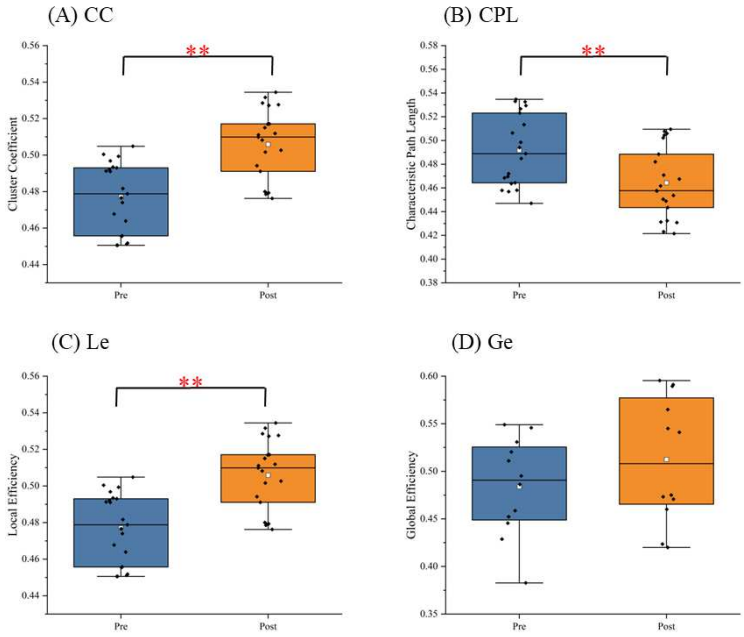


Fig. 8. Changes in network properties across 21 electrodes Pre- and Post- training (p < 0.01).**

IV. Discussion

This study employed MC, a time- and rhythm-based auditory symbolic system, as the stimulus, examined neural plasticity changes that occur as the brain transitions from a "novice" to a "proficient decoder." By integrating results from ERP, and brain networks, we systematically characterized how symbolic system learning modulates task-evoked brain information-processing patterns.

At the behavioral level, two months of MC training improved both ACC and RT in the experimental group: after training, participants decoded more accurately and responded more quickly, indicating increased efficiency in neural circuits involved in MC symbol processing and more effective information transmission and integration(Mai et al., 2024; Skoe & Kraus, 2024). The control group showed largely stable performance across the two measurement sessions, ruling out practice effects and natural maturation as alternative explanations and supporting the conclusion that behavioral improvements primarily stem from MC training itself. The marked Post-training improvement in the experimental group is consistent with the hypothesis proposed in the Introduction that learning a structured auditory symbolic system can induce experience-dependent neural plasticity within a relatively short time window(Tamminen et al., 2024).

At the electrophysiological level, the N200 component amplitude decreased after MC training (i.e., the negative

deflection was reduced), indicating that processing of MC symbols in the early information-processing stage became more efficient (as shown in Figures 5d and 5h). In light of cognitive automation theory, it can be inferred that as task proficiency increases, the extraction of MC acoustic and rhythmic features shifts from resource-demanding, controlled processing toward a more automated mode(Shiffrin & Schneider, 1977), reducing the need for conflict monitoring and error signaling and thereby decreasing N200 negativity(Botvinick & Braver, 2015; Houghton & Tipper, 1996). At the same time, theories of attentional bias and learning–memory suggest that training strengthens selective attention and memory representations for MC symbols, allowing participants to extract task-relevant information more rapidly and directly from the background without recruiting large amounts of additional cognitive resources(Shim et al., 2023). Thus, the reduction in N200 amplitude does not imply weaker processing; rather, it likely reflects more economical and efficient resource utilization in the domains of attention, control, and memory encoding(Pei et al., 2022). This finding provides support for Hypothesis 2 proposed in the Introduction.

At the brain network level, this study examined the impact of MC learning on the organization of neural information processing from three perspectives: lateralization, network topology, and hub nodes. The PLV difference network showed that post-training connectivity was globally enhanced in the right hemisphere, and the network exhibited a right-lateralized pattern(Zatorre et al., 2007; Harding et al., 2019). This pattern suggests that long-term training may induce remodeling of neural pathways, either by forming new neuronal connections or by strengthening existing one(Schlaffke et al., 2017; Schmidt-Wilcke et al., 2010). Quantitatively, a significant 412.3% reduction in *LI* ($p < 0.01$, Cohen's $d = -0.889$) was found in the training group, signaling a shift to right-hemispheric dominance, with no significant change in the control group. This pattern is consistent with previous findings on the advantages of the right hemisphere in temporal processing, rhythm perception, and non-lexical auditory symbolic processing(Limb et al., 2006; Riecker et al., 2002), and suggests that learning MC, as a time-rhythm-based symbolic system, drives a shift from relatively symmetric processing toward a right-hemisphere-dominant network organization(Tierney & Kraus, 2015). Graph-theoretical analyses further revealed that, within this right-lateralized network, the right temporal T8 node exhibited typical hub-like properties after training: the rankings of DC, NS, EC, and PC all improved, with three of these metrics entering the top 50% of all nodes. At the same time, connectivity between T8 and regions such as the prefrontal and occipital cortices was generally strengthened, indicating that T8 gradually evolved into a key hub for cross-regional information integration-coordinating, on the basis of auditory symbol encoding, attentional regulation and working memory in the prefrontal cortex, as well as rhythm/pattern perception in the occipital cortex(Harding et al., 2019). These findings consistently support that the T8 node exhibits prominent hub-like properties within the functional brain network.

In addition, MC training not only altered interhemispheric connectivity patterns and hub-node status, but also reshaped the global topological properties of the PLV network(Lou et al., 2025; Zhan et al., 2022). As shown in Figure 8, a significant increase in CC and Le points to enhanced local clustering and processing efficiency, while a significant decrease in CPL indicates optimized global integration. Despite not being statistically significant, the upward trend in Ge implies a concomitant improvement in global information transfer(Gu et al., 2023; J. Li et al., 2016; Lou et al., 2025; Zhan et al., 2022). Taken together, the *LI* results, the hub-like role of T8, and the network topological changes indicate that learning an auditory symbolic system such as MC not only promotes right-

hemisphere-biased reorganization of functional connectivity, but also enhances both local and global information-processing efficiency through T8-centered network reconfiguration, providing strong evidence for tracking the neural network reorganization process from “novice” to “proficient decoder” within a controlled symbolic system(J. Li et al., 2016; Zheng et al., 2022).One limitation of this study is that the relatively long training period and the specialized occupational sample restricted the sample size and task scope. Given the small sample size, we prioritized combining data across different code speeds to enhance statistical power, and thus, did not analyze the effects of varying code speeds on behavioral and neural outcomes. Additionally, while the task focused on symbol discrimination (dot counting), it did not involve full letter-level decoding. Therefore, the observed ERP and connectivity changes should be interpreted as task-specific modulations, rather than as a broad reorganization of neural architecture.

V. Conclusion

In this study, MC was used as the stimulus to characterize neural plasticity underlying the transition from “novice” to “proficient decoder” two complementary levels: the local level (ERP) and the global level (PLV). Two months of MC training significantly improved participants’ performance in rhythmic perception, supporting the notion that structured symbolic learning can induce brain plasticity within a relatively short period. The decrease in N200 amplitude indicated more efficient extraction of MC’s acoustic and rhythmic information, with reduced reliance on highly controlled processing and conflict monitoring, suggesting a shift toward more automated decoding. PLV-based analyses further revealed a rightward reorganization of functional connectivity, with the right temporal T8 node showing increased hub-like centrality, and network properties becoming more favorable for information integration and transmission. This study proposes a set of candidate neural markers for EEG-based auditory discrimination assessment. Future research will address the limitations of this study by examining how different code speeds influence neural dynamics and performance. We also plan to design experiments exploring the role of semantic processing in MC recognition, focusing on EEG-based decoding of the semantic aspects of auditory symbolic processing. These efforts will extend the results to larger, more diverse samples and tasks, incorporating multimodal imaging and online decoding techniques to assess the stability and real-world applicability of these neural markers.

Availability of Data and Materials

The data are available from the corresponding author upon reasonable request.

Author Contributions

Zhongyang He: Writing – review & editing, Writing – original draft, Visualization, Methodology, Investigation, Software, Formal analysis, Data curation, Conceptualization. Ying Zeng: Conceptualization, Writing – review & editing, Writing – original draft, Methodology, Funding acquisition. Hua Zhao: Writing – review & editing, Data curation. Li Tong: Writing – review & editing, Methodology, Conceptualization. Shan Gao and Yunying Qu: Writing – review & editing. Yuanlong Gao: Methodology, Investigation. Changfu Pei: Writing – review & editing, Writing – original draft, Methodology, Software, Formal analysis, Supervision. Bin Yan: Writing – review & editing, Funding acquisition, Supervision. All authors contributed to editorial changes in the manuscript. All authors read and approved

the final manuscript.

Ethics Approval and Consent to Participate

The study was conducted in accordance with the Declaration of Helsinki, and approved by the Ethics Committee of University of Electronic Science and Technology of China.

Acknowledgment

We would like to thank Professor Ying Li from Zhengzhou University and Lecturer Yajing Si from Henan University of Chinese Medicine for their valuable suggestions on revising the manuscript. We also extend our gratitude to our team members-Kunlin Guo, Siyuan Zhang, and Jian Zhang-for their insightful comments.

Fundings

This work is funded by Brain Science and Brain-like Intelligence Technology- National Science and Technology Major Project No.2022ZD0208500, in part by the National Natural Science Foundation of China (Grant No.62106285), and in part by the Central Plains Science and Technology Innovation Leading Talent Project (Grant No.244200510015).

Conflicts of Interest

The authors declare no conflict of interest.

References

Abrams, D. A., Nicol, T., Zecker, S., & Kraus, N. (2008). Right-hemisphere auditory cortex is dominant for coding syllable patterns in speech. *The Journal of Neuroscience: The Official Journal of the Society for Neuroscience*, *28*(15), 3958–3965. https://doi.org/10.1523/JNEUROSCI.0187-08.2008

Balconi, M., & Vanutelli, M. E. (2016). Hemodynamic (fNIRS) and EEG (N200) correlates of emotional inter-species interactions modulated by visual and auditory stimulation. *Scientific Reports*, *6*, 23083. https://doi.org/10.1038/srep23083

Botvinick, M., & Braver, T. (2015). Motivation and cognitive control: From behavior to neural mechanism. *Annual Review of Psychology*, *66*, 83–113. https://doi.org/10.1146/annurev-psych-010814-015044

Bullmore, E., & Sporns, O. (2009). Complex brain networks: Graph theoretical analysis of structural and functional systems. *Nature Reviews. Neuroscience*, *10*(3), 186–198. https://doi.org/10.1038/nrn2575

Chiang, K.-J., Dong, S., Cheng, C.-K., & Jung, T.-P. (2023). Using EEG signals to assess workload during memory retrieval in a real-world scenario. *Journal of Neural Engineering*, *20*(3). https://doi.org/10.1088/1741-2552/accbed

Crowley, K. E., & Colrain, I. M. (2004). A review of the evidence for P2 being an independent component process: Age, sleep and modality. *Clinical Neurophysiology*, *115*(4), 732–744. https://doi.org/10.1016/j.clinph.2003.11.021

Folstein, J. R., & Van Petten, C. (2008). Influence of cognitive control and mismatch on the N2 component of the ERP: A review. *Psychophysiology*, *45*(1), 152–170. https://doi.org/10.1111/j.1469-8986.2007.00602.x

Gu, H., Chen, H., Yao, Q., He, W., Wang, S., Yang, C., Li, J., Liu, H., Li, X., Zhao, X., Liang, G., Gu, H., Chen, H., Yao, Q., He, W., Wang, S., Yang, C., Li, J., Liu, H., … Liang, G. (2023). Efficiency of the Brain Network Is Associated with the Mental Workload with Developed Mental Schema. *Brain Sciences*, *13*(3). https://doi.org/10.3390/brainsci13030373

Harding, E. E., Sammler, D., Henry, M. J., Large, E. W., & Kotz, S. A. (2019). Cortical tracking of rhythm in music and speech. *NeuroImage*, *185*, 96–101. https://doi.org/10.1016/j.neuroimage.2018.10.037

Houghton, G., & Tipper, S. P. (1996). Inhibitory mechanisms of neural and cognitive control: Applications to selective attention and sequential action. *Brain and Cognition*, *30*(1), 20–43. https://doi.org/10.1006/brcg.1996.0003

Junker, F. B. (n.d.). *Morse Code – A Window on Language Decoding in the Brain*.

Klug, S., Godbersen, G. M., Rischka, L., Wadsak, W., Pichler, V., Klöbl, M., Hacker, M., Lanzenberger, R., & Hahn, A. (2022). Learning induces coordinated neuronal plasticity of metabolic demands and functional brain networks. *Communications Biology*, *5*(1), 428. https://doi.org/10.1038/s42003-022-03362-4

Kujala, A., Huotilainen, M., Uther, M., Shtyrov, Y., Monto, S., Ilmoniemi, R. J., & Näätänen, R. (2003). Plastic cortical changes induced by learning to communicate with non-speech sounds: *NeuroReport*, *14*(13), 1683–1687. https://doi.org/10.1097/00001756-200309150-00005

Li, F., Chen, B., Li, H., Zhang, T., Wang, F., Jiang, Y., Li, P., Ma, T., Zhang, R., Tian, Y., Liu, T., Guo, D., Yao, D., & Xu, P. (2016). The Time-Varying Networks in P300: A Task-Evoked EEG Study. *IEEE Transactions on Neural Systems and Rehabilitation Engineering*, *24*(7), 725–733. IEEE Transactions on Neural Systems and Rehabilitation Engineering. https://doi.org/10.1109/TNSRE.2016.2523678

Li, J., Lim, J., Chen, Y., Wong, K., Thakor, N., Bezerianos, A., & Sun, Y. (2016). Mid-Task Break Improves Global Integration of Functional Connectivity in Lower Alpha Band. *Frontiers in Human Neuroscience*, *10*. https://doi.org/10.3389/fnhum.2016.00304

Li, X., Salami, A., & Persson, J. (2023). Hub architecture of the human structural connectome: Links to aging and processing speed. *NeuroImage*, *278*, 120270. https://doi.org/10.1016/j.neuroimage.2023.120270

Limb, C. J., Kemeny, S., Ortigoza, E. B., Rouhani, S., & Braun, A. R. (2006). Left hemispheric lateralization of brain activity during passive rhythm perception in musicians. *The Anatomical Record. Part A, Discoveries in Molecular, Cellular, and Evolutionary Biology*, *288*(4), 382–389. https://doi.org/10.1002/ar.a.20298

Liu, C., Jiao, L., Timmer, K., & Wang, R. (2021). Structural brain changes with second language learning: A longitudinal voxel-based morphometry study. *Brain and Language*, *222*, 105015. https://doi.org/10.1016/j.bandl.2021.105015

Lou, Y., Pi, R., Sun, R., Wu, J., Wang, W., Zhu, Z., Dai, T., & Gong, W. (2025). Graph theory-based analysis of functional connectivity changes in brain networks underlying cognitive fatigue: An EEG study. *PloS One*, *20*(8), e0329212. https://doi.org/10.1371/journal.pone.0329212

Lövdén, M., Wenger, E., Mårtensson, J., Lindenberger, U., & Bäckman, L. (2013). Structural brain plasticity in adult learning and development. *Neuroscience & Biobehavioral Reviews*, *37*(9, Part B), 2296–2310.

https://doi.org/10.1016/j.neubiorev.2013.02.014

Luck, S. J. (2005). An Introduction to The Event-Related Potential Technique. *Sveučilište u Rijeci*. http://www.researchgate.net/publication/200003627_An_Introduction_to_The_Event-Related_Potential_Technique

Mai, G., Jiang, Z., Wang, X., Tachtsidis, I., & Howell, P. (2024). Neuroplasticity of Speech-in-Noise Processing in Older Adults Assessed by Functional Near-Infrared Spectroscopy (fNIRS). *Brain Topography*, *37*(6), 1139–1157. https://doi.org/10.1007/s10548-024-01070-2

Mankel, K., Shrestha, U., Tipirneni-Sajja, A., & Bidelman, G. M. (2022). Functional Plasticity Coupled With Structural Predispositions in Auditory Cortex Shape Successful Music Category Learning. *Frontiers in Neuroscience*, *16*, 897239. https://doi.org/10.3389/fnins.2022.897239

Murias, M., Webb, S. J., Greenson, J., & Dawson, G. (2007). Resting state cortical connectivity reflected in EEG coherence in individuals with autism. *Biological Psychiatry*, *62*(3), 270–273. https://doi.org/10.1016/j.biopsych.2006.11.012

Näätänen, R., & Picton, T. (1987). The N1 wave of the human electric and magnetic response to sound: A review and an analysis of the component structure. *Psychophysiology*, *24*(4), 375–425. https://doi.org/10.1111/j.1469-8986.1987.tb00311.x

Newman, M., & Newman, M. (2018). *Networks* (Second Edition, Second Edition). Oxford University Press.

Oechslin, M. S., Gschwind, M., & James, C. E. (2018). Tracking Training-Related Plasticity by Combining fMRI and DTI: The Right Hemisphere Ventral Stream Mediates Musical Syntax Processing. *Cerebral Cortex*, *28*(4), 1209–1218. https://doi.org/10.1093/cercor/bhx033

Panjeh, S., Nordahl-Hansen, A., & Cogo-Moreira, H. (2023). Establishing new cutoffs for Cohen's d: An application using known effect sizes from trials for improving sleep quality on composite mental health. *International Journal of Methods in Psychiatric Research*, *32*(3), e1969. https://doi.org/10.1002/mpr.1969

Patel, S. H., & Azzam, P. N. (2005). Characterization of N200 and P300: Selected studies of the Event-Related Potential. *International Journal of Medical Sciences*, *2*(4), 147–154. https://doi.org/10.7150/ijms.2.147

Pei, C., Huang, X., Li, Y., Chen, B., Lu, B., Peng, Y., Si, Y., Zhang, X., Zhang, T., Yao, D., Li, F., & Xu, P. (2022). Auditory Dominance in Processing Chinese Semantic Abnormalities in Response to Competing Audio-visual Stimuli. *Neuroscience*, *502*, 1–9. https://doi.org/10.1016/j.neuroscience.2022.08.017

Pei, C., Huang, X., Qiu, Y., Peng, Y., Gao, S., Biswal, B., Yao, D., Liu, Q., Li, F., & Xu, P. (2023). Frequency-specific directed interactions between whole-brain regions during sentence processing using multimodal stimulus. *Neuroscience Letters*, *812*, 137409. https://doi.org/10.1016/j.neulet.2023.137409

Pei, C., Qiu, Y., Li, F., Huang, X., Si, Y., Li, Y., Zhang, X., Chen, C., Liu, Q., Cao, Z., Ding, N., Gao, S., Alho, K., Yao, D., & Xu, P. (2023). The different brain areas occupied for integrating information of hierarchical linguistic units: A study based on EEG and TMS. *Cerebral Cortex (New York, N.Y.: 1991)*, *33*(8), 4740–4751. https://doi.org/10.1093/cercor/bhac376

Pion-Tonachini, L., Kreutz-Delgado, K., & Makeig, S. (2019). ICLabel: An automated electroencephalographic independent component classifier, dataset, and website. *NeuroImage*, *198*, 181–197.

https://doi.org/10.1016/j.neuroimage.2019.05.026

Riecker, A., Wildgruber, D., Dogil, G., Grodd, W., & Ackermann, H. (2002). Hemispheric Lateralization Effects of Rhythm Implementation during Syllable Repetitions: An fMRI Study. *NeuroImage*, *16*(1), 169–176. https://doi.org/10.1006/nimg.2002.1068

Rubinov, M., & Sporns, O. (2010). Complex network measures of brain connectivity: Uses and interpretations. *NeuroImage*, *52*(3), 1059–1069. https://doi.org/10.1016/j.neuroimage.2009.10.003

Schlaffke, L., Leemans, A., Schweizer, L. M., Ocklenburg, S., & Schmidt-Wilcke, T. (2017). Learning morse code alters microstructural properties in the inferior longitudinal fasciculus: A DTI study. *Frontiers in Human Neuroscience*, *11*, undefined-undefined. https://doi.org/10.3389/fnhum.2017.00383

Schlaffke, L., Rüther, N. N., Heba, S., Haag, L. M., Schultz, T., Rosengarth, K., Tegenthoff, M., Bellebaum, C., & Schmidt-Wilcke, T. (2015). From perceptual to lexico-semantic analysis—Cortical plasticity enabling new levels of processing. *Human Brain Mapping*, *36*(11), 4512–4528. https://doi.org/10.1002/hbm.22939

Schmidt-Wilcke, T., Rosengarth, K., Luerding, R., Bogdahn, U., & Greenlee, M. W. (2010). Distinct patterns of functional and structural neuroplasticity associated with learning Morse code. *NeuroImage*, *51*(3), 1234–1241. https://doi.org/10.1016/j.neuroimage.2010.03.042

Seghier, M. L. (2008). Laterality index in functional MRI: Methodological issues. *Magnetic Resonance Imaging*, *26*(5), 594–601. https://doi.org/10.1016/j.mri.2007.10.010

Shiffrin, R. M., & Schneider, W. E. (1977). Controlled and automatic human information processing: I. Detection, search, and attention. *Psychological Review*, *84*(2), N/A. https://doi.org/10.1037%25252F0033-295X.84.1.1

Shim, H., Gibbs, L., Rush, K., Ham, J., Kim, S., Kim, S., & Choi, I. (2023). Neural Mechanisms Related to the Enhanced Auditory Selective Attention Following Neurofeedback Training: Focusing on Cortical Oscillations. *Applied Sciences (Basel, Switzerland)*, *13*(14), 8499. https://doi.org/10.3390/app13148499

Skoe, E., & Kraus, N. (2024). Neural Delays in Processing Speech in Background Noise Minimized after Short-Term Auditory Training. *Biology*, *13*(7), 509. https://doi.org/10.3390/biology13070509

Song, C., Zhang, J., Liu, Y., Hu, Y., Feng, C., Shi, P., Zhang, Y., Wang, L., Xie, Y., Zhang, M., Zhao, X., Cao, Y., Li, C., & Sun, H. (2022). Characterization and Validation of ceRNA-Mediated Pathway-Pathway Crosstalk Networks Across Eight Major Cardiovascular Diseases. *Frontiers in Cell and Developmental Biology*, *10*, 762129. https://doi.org/10.3389/fcell.2022.762129

Tamminen, H., Kujala, T., & Peltola, M. S. (2024). Training non-native speech sounds results in long-lasting plastic changes – Hard-wiring new memory traces takes time. *Lingua*, *302*, 103697. https://doi.org/10.1016/j.lingua.2024.103697

Tierney, A., & Kraus, N. (2015). Neural entrainment to the rhythmic structure of music. *Journal of Cognitive Neuroscience*, *27*(2), 400–408. https://doi.org/10.1162/jocn_a_00704

Uther, M., Kujala, A., Huotilainen, M., Shtyrov, Y., & Näätänen, R. (2006). Training in Morse code enhances involuntary attentional switching to acoustic frequency: Evidence from ERPs. *Brain Research*, *1073–1074*, 417–424. https://doi.org/10.1016/j.brainres.2005.12.047

Xu, P., Xiong, X. C., Xue, Q., Tian, Y., Peng, Y., Zhang, R., Li, P. Y., Wang, Y. P., & Yao, D. Z. (2014). Recognizing

mild cognitive impairment based on network connectivity analysis of resting EEG with zero reference. *Physiological Measurement*, *35*(7), 1279–1298. https://doi.org/10.1088/0967-3334/35/7/1279

Yao, D. (2001). A method to standardize a reference of scalp EEG recordings to a point at infinity. *Physiological Measurement*, *22*(4), 693–711. https://doi.org/10.1088/0967-3334/22/4/305

Yao, D., Qin, Y., Hu, S., Dong, L., Bringas Vega, M. L., & Valdés Sosa, P. A. (2019). Which Reference Should We Use for EEG and ERP practice? *Brain Topography*, *32*(4), 530–549. https://doi.org/10.1007/s10548-019-00707-x

Zatorre, R. J., Chen, J. L., & Penhune, V. B. (2007). When the brain plays music: Auditory-motor interactions in music perception and production. *Nature Reviews. Neuroscience*, *8*(7), 547–558. https://doi.org/10.1038/nrn2152

Zhan, G., Chen, S., Ji, Y., Xu, Y., Song, Z., Wang, J., Niu, L., Bin, J., Kang, X., & Jia, J. (2022). EEG-Based Brain Network Analysis of Chronic Stroke Patients After BCI Rehabilitation Training. *Frontiers in Human Neuroscience*, *16*, 909610. https://doi.org/10.3389/fnhum.2022.909610

Zhang, X., Jiang, Y., Zhang, S., Li, F., Pei, C., He, G., Ao, M., Yao, D., Zhao, Y., & Xu, P. (2021). Correlation Analysis of EEG Brain Network With Modulated Acoustic Stimulation for Chronic Tinnitus Patients. *IEEE Transactions on Neural Systems and Rehabilitation Engineering*, *29*, 156–162. https://doi.org/10.1109/TNSRE.2020.3039555

Zheng, R., Wang, Z., He, Y., & Zhang, J. (2022). EEG-based brain functional connectivity representation using amplitude locking value for fatigue-driving recognition. *Cognitive Neurodynamics*, *16*(2), 325–336. https://doi.org/10.1007/s11571-021-09714-w

Zou, Y., Tsang, Y.-K., & Wu, Y. (2019). Semantic Radical Activation in Chinese Phonogram Recognition: Evidence from Event-Related Potential Recording. *Neuroscience*, *417*, 24–34. https://doi.org/10.1016/j.neuroscience.2019.08.008

Appendix

A. Lateralization Index Calculation Method

To assess the lateralization of brain networks, we calculate the average functional connectivity of the left and right sides and perform statistical analysis.

- **Left-side connectivity average (*L*)**
- **Right-side connectivity average (*R*)**

The Lateralization Index (*LI*) is defined as:

$$LI = \frac{L - R}{L + R} \tag{1}$$

The lateralization is interpreted as follows:

- ***LI* > 0**: Left-side connectivity is stronger

- ***LI* < 0**: Right-side connectivity is stronger
- ***LI* = 0**: No significant lateralization

Statistical tests for each participant's *LI* are performed using paired t-tests and effect size (Cohen's d) analysis to assess the degree of network lateralization, and the calculation formula is as follows:

$$\text{Cohen's d} = \frac{mean_LI2 - mean_LI1}{\sqrt{\frac{(std_LI2)^2 + (std_LI1)^2}{2}}} \tag{2}$$

Among them, $mean_LI1$, $mean_LI2$, std_LI1, std_LI2, represent the means and standard deviations from the two measurements, respectively.

B. Graph Property Calculation Method

To comprehensively analyze the topological properties of brain functional networks, we employed several graph-theoretical metrics to quantify the connectivity and importance of nodes. Below are the methods for calculating the main graph properties:

1. Degree Centrality (DC)

Degree centrality measures the extent to which a node is connected to other nodes in the network. In weighted networks, degree centrality is the sum of the weights of all the edges connected to the node.

Formula:

$$DC_i = \sum_{j=1}^{N} w_{ij} \tag{3}$$

Where w_{ij} is the connection weight between node i and node j, and $N$is the total number of nodes in the network.

2. Node Strength (NS)

Node strength is a standardized version of degree centrality, where the degree centrality is divided by the maximum possible number of connections (i.e., the number of nodes minus 1), resulting in a value between 0 and 1. This makes it easier to compare networks of different sizes.

Formula:

$$NS_i = \frac{DC_i}{N-1} = \frac{\sum_{j \in N} w_{ij}}{N-1} \tag{4}$$

Where w_{ij} is the connection weight between node i and node j, and N is the total number of nodes in the network.

3. Betweenness Centrality (BC)

Betweenness centrality measures the importance of a node as a "bridge" in the network, indicating how many shortest paths pass through the node. In weighted networks, the shortest paths are typically calculated based on

distance (the inverse of the weight).

Formula:

$$BC_i = \sum_{s \neq i \neq t} \frac{\sigma_{st}(i)}{\sigma_{st}} \tag{5}$$

Where σ_{st} is the number of shortest paths between nodes s and t, and $\sigma_{st}(i)$ is the number of shortest paths passing through node i.

4. Eigenvector Centrality (EC)

Eigenvector centrality measures the importance of a node by considering not only the number of its neighbors but also the importance of those neighbors. A node with high eigenvector centrality is connected to many important nodes.

Formula:

$$\lambda v_i = \sum_{j=1}^{N} w_{ij} v_{ij} \tag{6}$$

Where A_{ij} is the adjacency matrix representing the connection between node i and node j, λ is the eigenvalue, and EC_i is the eigenvector centrality of node i. Typically, the eigenvector corresponding to the largest eigenvalue is used for calculating centrality.

5. Participation Coefficient (PC)

The participation coefficient measures the distribution of a node's connections across different communities (modules). A high participation coefficient indicates that the node connects multiple different communities, playing a role in integration.

Formula:

$$PC_i = 1 - \sum_{m=1}^{M} \left(\frac{k_i(m)}{k_i}\right)^2 \tag{7}$$

Where k_i is the degree of node i, k_{im} is the sum of the connection weights between node i and the nodes in community m, and M is the total number of communities (e.g., left hemisphere, right hemisphere, and midline).

C. Network Attributes Calculation Method

We calculated the network attributes for each participant based on the PLV connection matrices. These attributes included:

1.Clustering Coefficient (CC)

The CC quantifies the extent to which the neighbors of a node are interconnected, reflecting the network's local segregation or modular organization.

2.Characteristic Path Length (CPL)

CPL measures the average shortest path length between all node pairs, reflecting the global communication efficiency of the network, with shorter path lengths suggesting more efficient communication between distant regions.

3.Global Efficiency (Ge)

Ge is defined as the average inverse shortest path length between all node pairs, which captures the network's ability to exchange information across long distancess

4.Local Efficiency (Le)

Le evaluates the fault tolerance and information-processing efficiency of a node's immediate neighborhood after removing that node, which reflects the efficiency of information processing within local subnetworks and indicates network robustness under disruption.

The calculation methods for the four network properties are as follows (Zhang et al., 2021):

$$CC = \frac{1}{\mathrm{T}} \sum_{i \in N} \frac{\sum_{j,l \in N} \left(w_{ij} w_{il} w_{jj} \right)^{1/3}}{\sum_{j \in N} w_{ij} \left(\sum_{j \in N} w_{ij} - 1 \right)} \tag{8}$$

$$CPL = \frac{1}{T} \sum_{i \in N} \frac{\sum_{i \in N, j \neq i} d_{ij}}{T - 1} \tag{9}$$

$$Le = \frac{1}{T} \sum_{i \in N} \frac{\sum_{j,l \in N, j \neq i} \left(w_{ij} w_{il} [d_{jl}(N_i)]^{-1} \right)^{1/3}}{\sum_{j \in N} w_{ij} \left(\sum_{j \in N} w_{ij} - 1 \right)} \tag{10}$$

$$Ge = \frac{1}{T} \sum_{i \in N} \frac{\sum_{j \in N, j \neq i} \left(d_{ij} \right)^{-1}}{N - 1} \tag{11}$$

Where d_{ij} is the shortest weighted characteristic path length between *i* and *j*, w_{ij} is the coherence coefficient between channel *i* and channel *j;* coherence represents the linear relationship between two different channel signals in a specific frequency domain. *T* is the number of nodes, and *N* is the set of all nodes in a single experimental network.